

## Supporting Information

### **Multi-layered composite assembly of Bi nanospheres anchored on nitrogen-doped carbon nanosheets for ultrastable sodium storage**

Xinxin Wang,<sup>a</sup> Yang Wu,<sup>a</sup> Peng Huang,<sup>a</sup> Peng Chen,<sup>a</sup> Zuyong Wang,<sup>a</sup> Xiongwen Xu,<sup>b</sup> Jian Xie,<sup>c</sup> Ji Yan,<sup>d</sup> Shuigen Li,<sup>e</sup> Jian Tu<sup>\*, b</sup> and Yuan-Li Ding<sup>\*, a, c, f</sup>

<sup>a</sup> College of Materials Science and Engineering, Hunan University, Changsha, 410082, China

<sup>b</sup> LI FUN Technol Corp Ltd, Zhuzhou 412000, China

<sup>c</sup> State Key Lab of Silicon Materials, School of Materials Science and Engineering, Zhejiang University, Hangzhou, 310027, China

<sup>d</sup> School of Material and Chemical Engineering, Zhengzhou University of Light Industry, Zhengzhou, 450002, China

<sup>e</sup> School of New Energy Science and Engineering, Xinyu University, Xinyu, 338004, China

<sup>f</sup> College of Materials and Chemical Engineering, Hubei Provincial Collaborative Innovation Center for New Energy Microgrid, Key Laboratory of Inorganic Nonmetallic Crystalline and the Energy Conversion Materials, China Three Gorges University, Yichang, 443002, China

\* Corresponding authors:

Yuan-Li Ding ([ylding@hnu.edu.cn](mailto:ylding@hnu.edu.cn));

Jian Tu ([kenttu@lifuntech.com](mailto:kenttu@lifuntech.com))

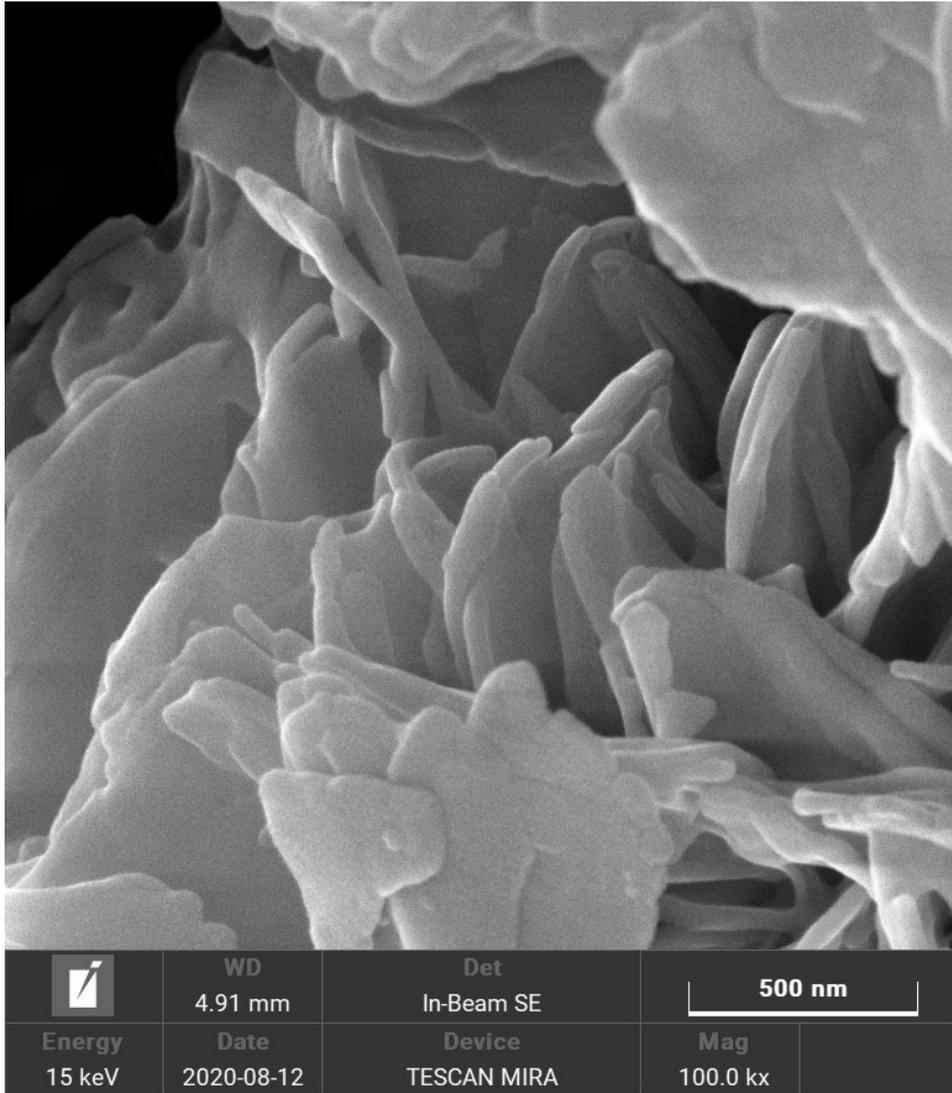


**Figure S1.** The SEM images of the precursor of ML-Bi@NCSs.

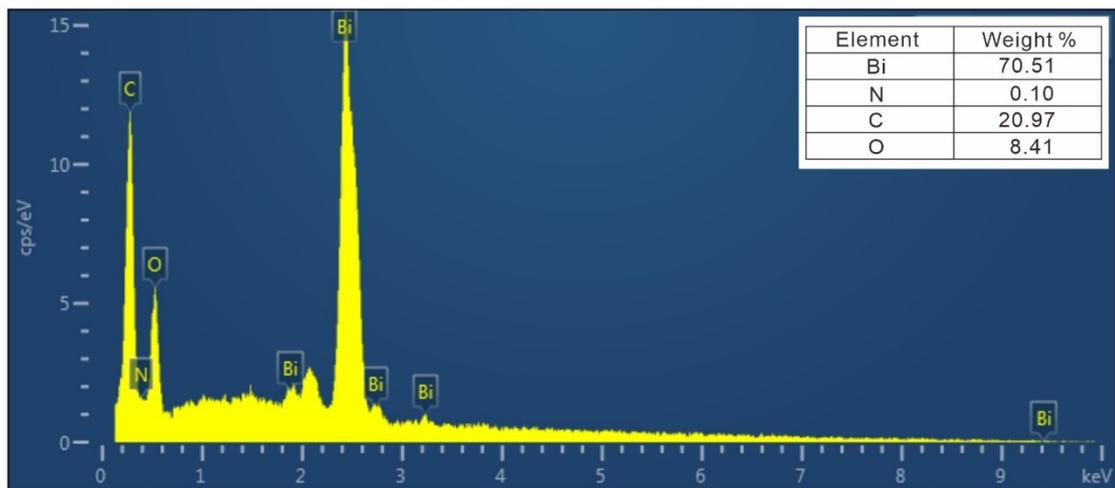


**Figure S2.** EDS patterns from SEM of ML-Bi@NCSs.

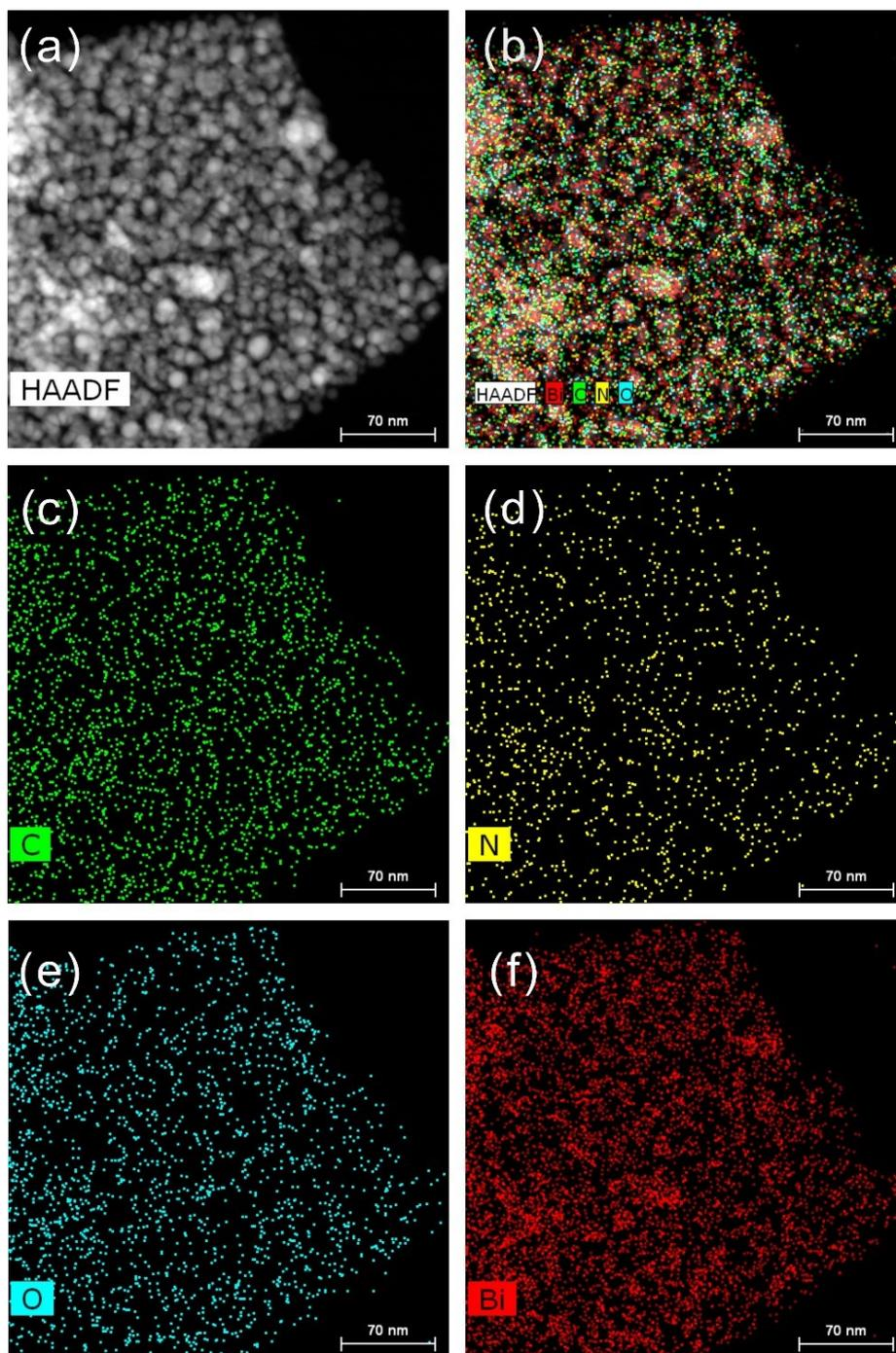


**Figure S3.** EDS mapping images (a-f) of from TEM of single layered ML-Bi@NCSs.

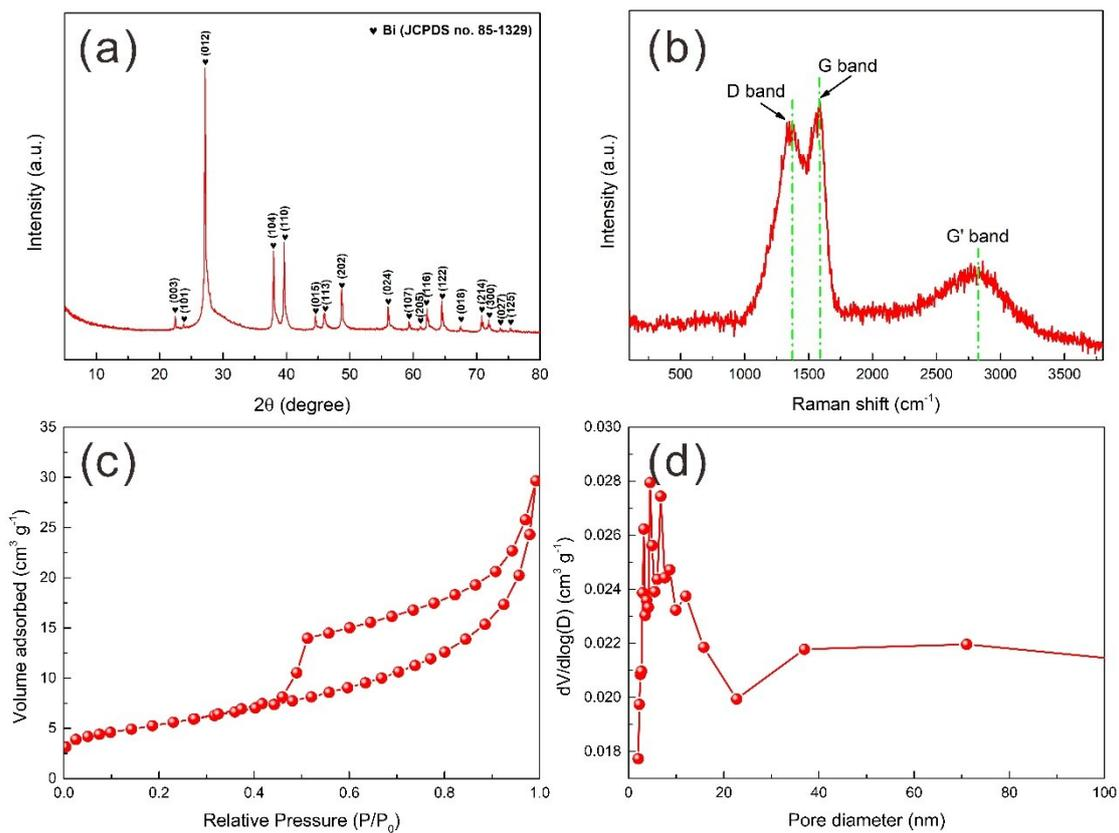


**Figure S4.** (a) XRD patterns and (b) Raman spectroscopy of ML-Bi@NCSs; The N<sub>2</sub> adsorption-desorption isotherms and the pore size distribution curve of Bi NPs/NC (c, d) and ML-Bi@NCSs (e, f) sample.

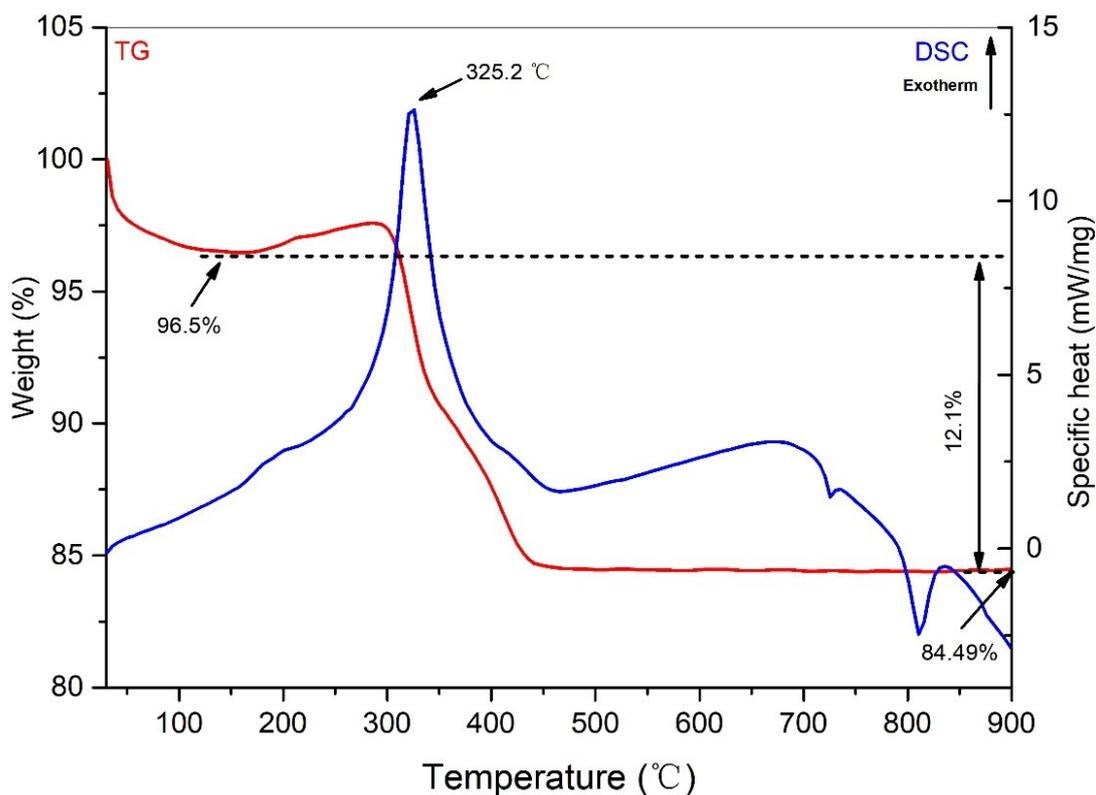


**Figure S5.** TGA and DSC curves of ML-Bi@NCSs in air (30-900 °C).

***The calculation process of weight ratio of N and C content:***

$$N \text{ and } C \text{ (wt\%)} = \left(1 - \frac{2 \times W_{Bi}}{W_{Bi_2O_3}} \times \frac{w_2}{w_1}\right) \times 100 \quad (1)$$

Where  $W_{Bi}$ ,  $W_{Bi_2O_3}$ ,  $w_1$  and  $w_2$  are the molecular mass of Bi, the molecular mass of  $Bi_2O_3$ , the initial weight ratio of ML-Bi@NCSs (%) about 100°C and the final weight ratio of  $Bi_2O_3$  (%) at 900°C, respectively.

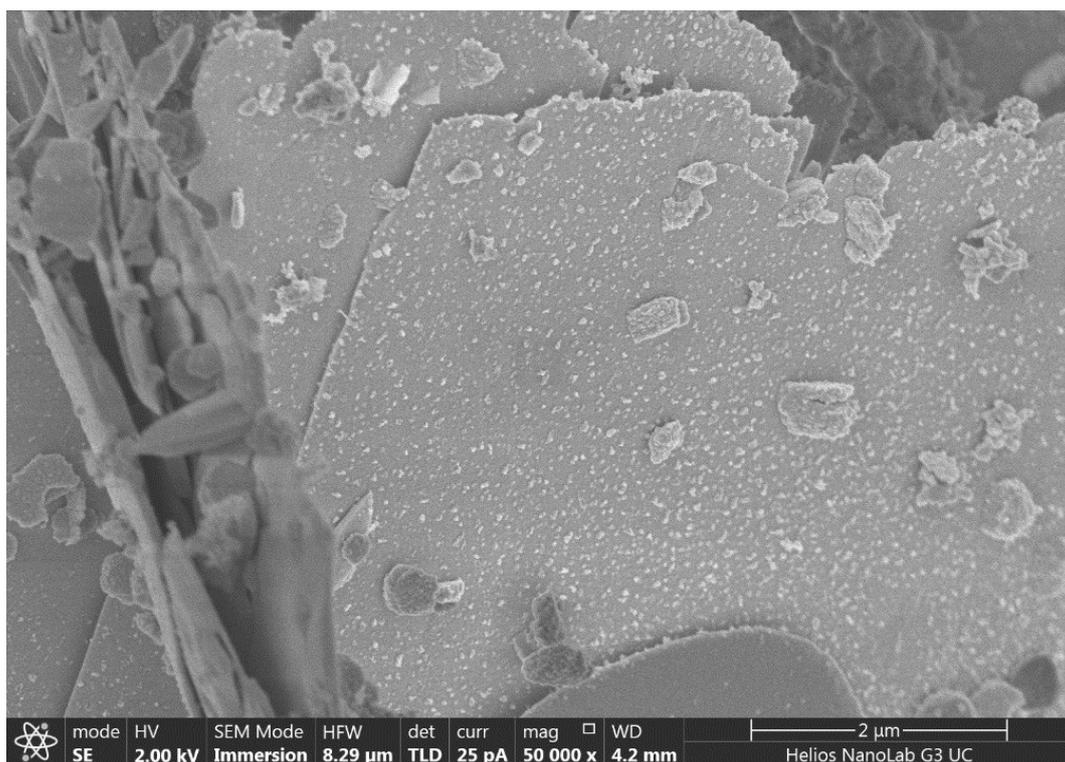


**Figure S6.** The SEM images of comparative sample of Bi NPs/NC.

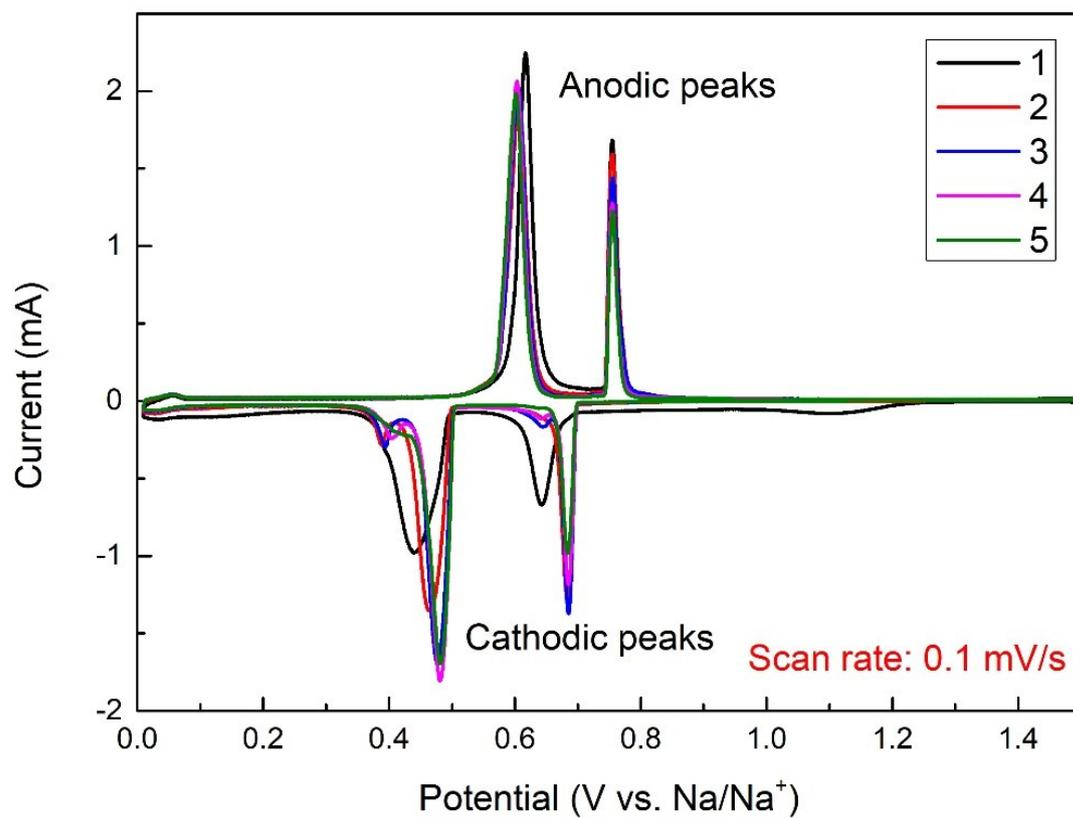


**Figure S7.** The CV curves at scan rate of  $0.1 \text{ mV s}^{-1}$  between 0.1 and 1.5 V of the Bi NPs/NC electrode.



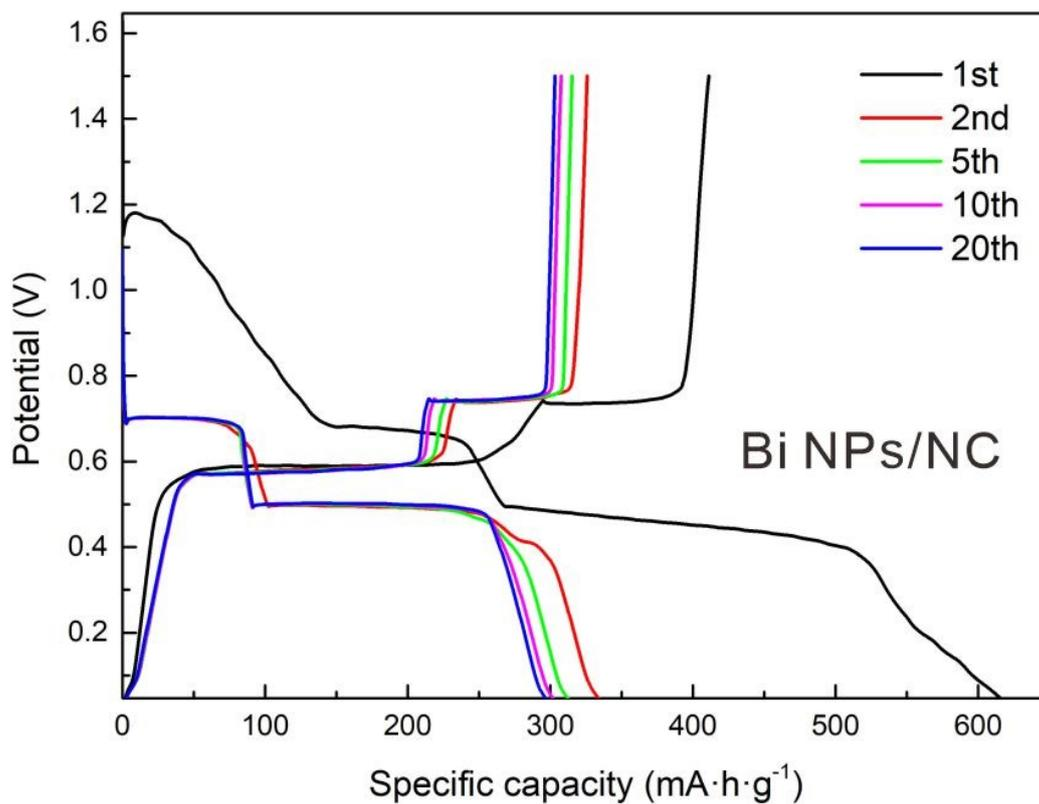


**Figure S8.** Galvanostatic charge-discharge curves at current density of 0.2 A g<sup>-1</sup> of the Bi NPs/NC electrode.

***The analytical process of reaction kinetics mode:***

The reaction kinetics mode was analyzed by the following equation and finite deformation:<sup>1, 2</sup>

$$I = av^b \quad (2)$$

$$\log(I) = b \log(v) + \log(a) \quad (3)$$

Where  $I$  and  $v$  are the peak current (mA) and sweep rate (mV s<sup>-1</sup>), respectively.  $b$  and  $a$  are two parameters.

***The detailed calculation process of contribution ratios of surface capacitive behavior:***

The contribution ratios of surface capacitive behavior were estimated with the following equation and finite deformation:<sup>2, 3</sup>

$$I(V) = k_1v + k_2v^{0.5} \quad (4)$$

$$I(V)/v^{0.5} = k_1v^{0.5} + k_2 \quad (5)$$

Where  $I$ ,  $V$  and  $v$  are the current (mA), corresponding voltage (mV) and sweep rate (mV s<sup>-1</sup>), respectively.  $k_1$  and  $k_2$  are constants, which can be calculated by current values at each given voltage on the CV curves and different sweep rate after linear fitting (Equation S4).  $k_1v$  and  $k_2v^{0.5}$  in Equation S3 are corresponding to the contribution of the surface capacitive behavior and diffusion-controlled process.

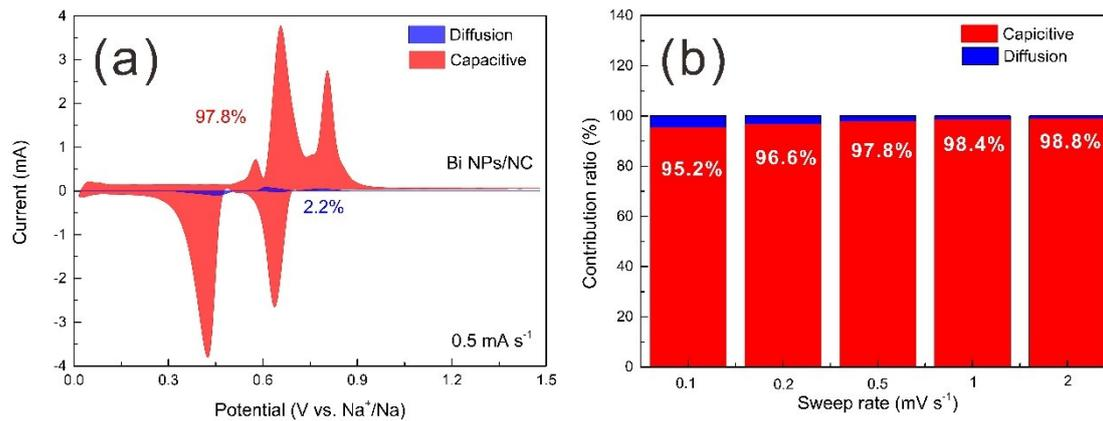


**Figure S9** (a) Capacitive contribution of Bi NPs/NC electrode at the sweep rate of 0.5 mV s<sup>-1</sup>; (b) Contribution ratio of capacitive behavior of Bi NPs/NC electrode at different sweep rate.

***The detailed calculation process of the diffusion coefficients ( $D_{Na^+}$ ) by CV measurements:***

The diffusion coefficients ( $D_{Na^+}$ ) were calculated by CV measurements based on Randles-Sevcik equation:<sup>4-6</sup>

$$I_p = 2.69 \times 10^5 n^{1.5} A C_0 D_{Na^+}^{0.5} \nu^{0.5} \quad (6)$$

Where  $I_p$  is the peak current (A),  $n$  is the number of electrons,  $A$  is the electrode surface area ( $\text{cm}^2$ ),  $C_0$  is the ion concentration of the electrolyte on the surface of the electrode ( $\text{mol cm}^{-3}$ ),  $\nu$  is the sweep rate ( $\text{V s}^{-1}$ ),  $D_{Na^+}$  is the diffusion coefficient ( $\text{cm}^2 \text{s}^{-1}$ ).

The detailed calculation process of the diffusion coefficients ( $D_{Na^+}^{GITT}$ ) in GITT:

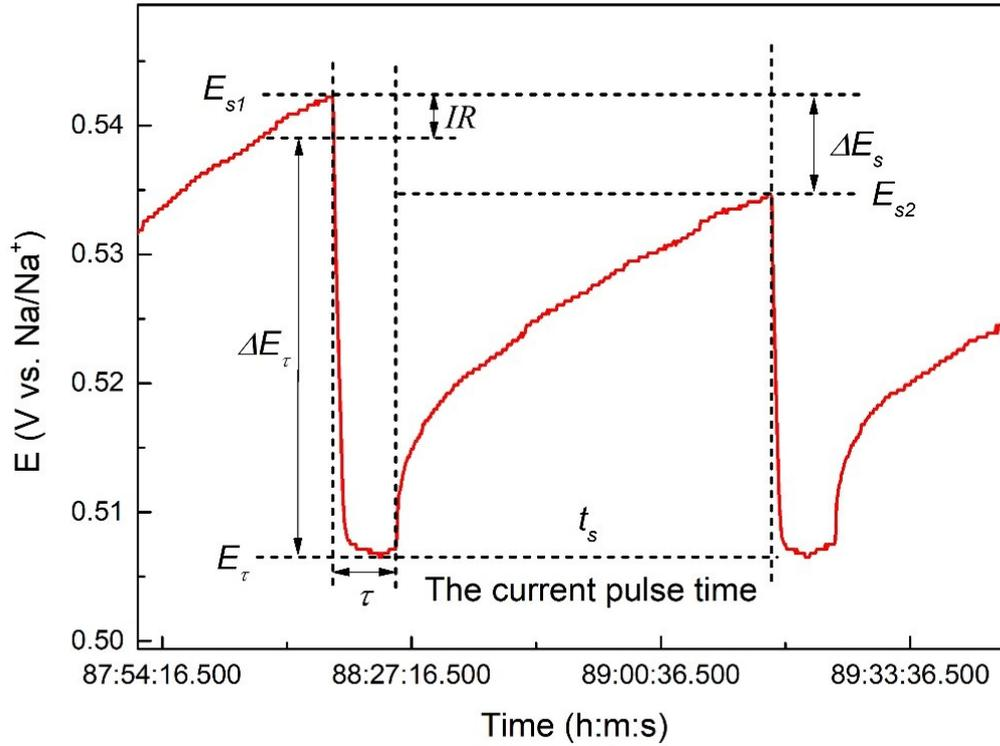


**Figure S10** Potential vs. time curves of ML-Bi@NCSs electrode for a single GITT during discharge process.

The diffusion coefficients ( $D_{Na^+}^{GITT}$ ) in galvanostatic intermittent titration technique (GITT) were calculated based on the following equation:<sup>7, 8</sup>

$$D_{Na^+}^{GITT} = \frac{4}{\pi\tau} \left( \frac{m_B V_M}{M_B S} \right)^2 \left( \frac{\Delta E_s}{\Delta E_\tau} \right)^2 \quad (7)$$

where  $\tau$  is the constant current pulse time (s),  $m_B$  is the mass (g),  $V_M$  is the molar volume ( $\text{cm}^3 \text{mol}^{-1}$ ),  $M_B$  is the molar mass ( $\text{g mol}^{-1}$ ),  $S$  is the contact area between the electrode and electrolyte ( $\text{cm}^2$ );  $\Delta E_s$  is the steady-state potential change (V) by the current pulse,  $\Delta E_\tau$  is the potential change (V) during the constant current pulse (s) after eliminating the  $IR$  drop (Figure S10).

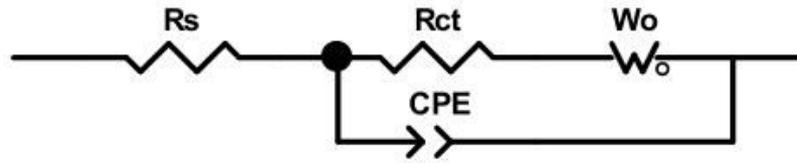


**Figure S11.** Equivalent circuit of the EIS fitting for ML-Bi@NCSs electrode.

**Note:**  $R_s$ : the ohmic resistance;  $R_{ct}$ : the charge transfer resistance;  $CPE$ : the constant phase element of charge transfer;  $W_o$ : the Warburg impedance related to the diffusion of sodium ions into the bulk electrode.

**Table S1.** The fitting data of the electrochemical impedance spectroscopy (EIS) for the Bi NPs/NC and ML-Bi@NCSs electrode from Figure 5a-d.

Cycle	Electrode	$R_s$ ( $\Omega$ )	$R_{ct}$ ( $\Omega$ )	CPE		$W_o$		
				CPE-T	CPE-P	W-R	W-T	W-P
Fresh	Bi NPs/NC	26.94	102.9	$1.0154 \times 10^{-5}$	0.62561	258140	102.4	0.64149
	ML-Bi@NCSs	33.01	62.11	$7.9302 \times 10^{-5}$	0.61028	46744	77.48	0.70339
1st	Bi NPs/NC	8.786	7	$8.866 \times 10^{-5}$	0.7321	19193	146	0.68271
	ML-Bi@NCSs	2.01	1.7	$3.3736 \times 10^{-5}$	0.87	15.7	0.25127	0.395
100th	Bi NPs/NC	1.52	1.58	$8.926 \times 10^{-5}$	0.82013	19468	127.8	0.80392
	ML-Bi@NCSs	1.45	1.13	$9.8561 \times 10^{-5}$	0.87144	997.9	1083	0.62853
3000th	Bi NPs/NC	2.864	16.5	0.000253	0.67187	5286	5500	0.555
	ML-Bi@NCSs	1.611	0.2445	0.005203	0.55608	0.20358	0.0003579	0.37357

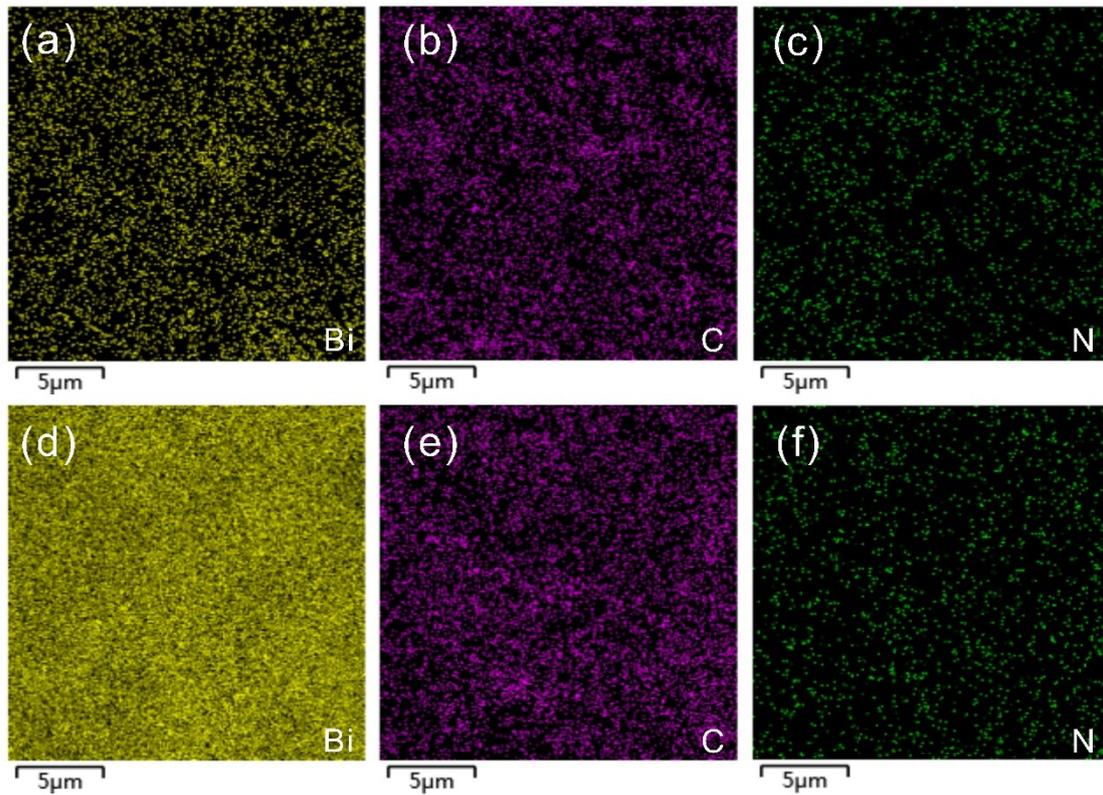


**Figure S12.** The EDS mapping (Bi, C, N) of Bi NPs/NC (a-c) and ML-Bi@NCSs electrode (d-f) after 3,500 cycles at  $5 \text{ A g}^{-1}$ .



## References

- 1 J. Chen, X. L. Fan, X. Ji, T. Gao, S. Hou, X. Q. Zhou, L. N. Wang, F. Wang, C. Y. Yang, L. Chen and C. S. Wang, *Energy Environ. Sci.*, 2018, **11**, 1218-1225.
- 2 P. Lu, Y. Sun, H. F. Xiang, X. Liang and Y. Yu, *Adv. Energy Mater.*, 2018, **8**, 1702434.
- 3 X. Y. Li, K. K. Li, S. C. Zhu, K. Fan, L. L. Lyu, H. M. Yao, Y. Y. Li, J. L. Hu, H. T. Huang, Y. W. Mai and J. B. Goodenough, *Angew. Chem., Int. Ed.*, 2019, **58**, 6239-6243.
- 4 X. L. Cheng, D. J. Li, Y. Wu, R. Xu and Y. Yu, *J. Mater. Chem. A*, 2019, **7**, 4913-4921.
- 5 X. X. Wang, H. M. Jian, Q. Xiao and S. P. Huang, *Appl. Surf. Sci.*, 2018, **459**, 40-47.
- 6 J. R. Dahn, J. W. Jiang, L. M. Moshurchak, M. D. Fleischauer, C. Buhrmester and L. J. Krause, *J Electrochem Soc*, 2005, **152**, A1283-A1289.
- 7 L. B. Wang, A. A. Voskanyan, K. Y. Chan, B. Qin and F. J. Li, *ACS Appl. Energy Mater.*, 2020, **3**, 565-572.
- 8 G. Z. Fang, Z. X. Wu, J. Zhou, C. Y. Zhu, X. X. Cao, T. Q. Lin, Y. M. Chen, C. Wang, A. Q. Pan and S. Q. Liang, *Adv. Energy Mater.*, 2018, **8**, 1703155.